High energy spectroscopy on vanadium oxides

Pen, Hermen Folken

Chapter 7

Kondo-lattice-like effects of hydrogen in transition metals

This chapter is based on a manuscript by R. Eder, H.F. Pen and G.A. Sawatzky, accepted for publication in Physical Review B **56** (1997).

Abstract

We discuss the possibility of a Kondo like effect associated with H in metals resulting from the strong dependence of the H-1s orbital radius on the occupation number. Such a strong breathing property of the orbital radius translates directly into a strong occupation-dependent hopping. It results in the formation of local singlet-like bound states involving one electron on H and one on the surrounding metal orbitals. Already at a mean field level, an occupation-dependent hopping integral leads to a substantial potential energy correction on hydrogen. The failure of band structure methods to incorporate this correction is responsible for the incorrect prediction of a metallic ground state for the YH_3 switchable mirror compounds.

7.1 Introduction

The recent discovery [1] of the so-called switchable mirror compounds based on YH_{3-x} has renewed the interest in the electronic structure of transition metal and rare earth hydrides. The study of YH_{3-x} has long hampered by its reactivity. Huiberts *et al.* circumvented this problem by coating a bulk yttrium sample with a thin palladium layer, which protects the yttrium from oxidation but which is permeable by hydrogen. By applying atmospheric H_2 pressure it became clear that YH_{3-x} undergoes a metal to insulator transition as x changes from one to zero, accompanied by a pronounced change in the optical properties. The metallic phase shows a high optical reflectivity, while the insulator is transparent for photon energies below about 2 eV. Band structure calculations within the local density approximation (LDA) fail to reproduce the semiconducting gap for $x = 3$ in either the cubic LaH_3 structure or the HoD_3

structure [2, 3], of which the latter was determined from neutron diffraction experiments [4, 5]. A gap can be obtained for more complicated distorted structures [6], but it is still much too small. And although such distortions are not excluded for YH_3, they do not appear to occur for LaH_3: the properties of this compound suggest also a band gap of $\gtrsim 2$ eV [1, 7], while LDA calculations predict LaH_3 to be a metal [3, 8, 9] or a small gap semiconductor [10].

The failure to produce large enough band gaps in semiconductors by LDA is a well-known shortcoming, which here however seems to take quite dramatic forms: the valence and conduction bands in LDA overlap by about 1 eV, so a total relative shift of about 3 eV is required to match the experimental value. Such large discrepancies are reminiscent of the strongly correlated systems like the transition metal and rare earth oxides and point perhaps to the importance of correlation effects. Since however the H-1s orbitals are rather extended as compared to the 3d orbitals of the transition metals, especially for the negative ion, they are expected to form rather broad bands, and the on-site Coulomb interactions are strongly screened. Therefore, the origin of the correlation effects may be quite different. Here, we address this problem and come to the new suggestion that the correlation effects are a consequence of the large change in the H-1s orbital radius upon orbital occupation. This "breathing" property of the hydrogen ion introduces a new term in the mean field treatment of the electronic structure of hydrides. This term results in an opening of the band gap in a quite natural way, with the retention of large bandwidths and nearly one particle behaviour of the excited states. Using a model Hamiltonian to demonstrate this behaviour we also show that for a range of parameter values the system behaves like a Kondo lattice insulator similar to that suggested by Ng *et al* [11].

7.2 The breathing hydrogen atom

As is well known and referred to in most general chemistry text books, the so called effective radius of hydrogen is extremely strongly dependent on the charge state. The crystal radius of neutral H is 0.26 Å, whereas that of the negative ion H^- is 1.54 Å [12]. The values of the average 1s orbital radius $\sqrt{<r^2>}$, as obtained from free ion Hartree-Fock calculations, are 0.8 Å for H and 1.72 Å for H^- [13]. This very large change is not unexpected since in H, with its low nuclear charge of one, the screening of the nuclear Coulomb potential by a second s electron is very important and greatly affects the orbital radius. This large effect causes the effective hopping integrals or hybridizations with surrounding ions to be strongly different for the fluctuations involving H to H^+ as compared to those involving H to H^-, as pictured in Fig. 7.1. If these instantaneous changes in the hopping integrals are larger than or comparable to other energy scales, like the orbital energy splittings, they must be treated

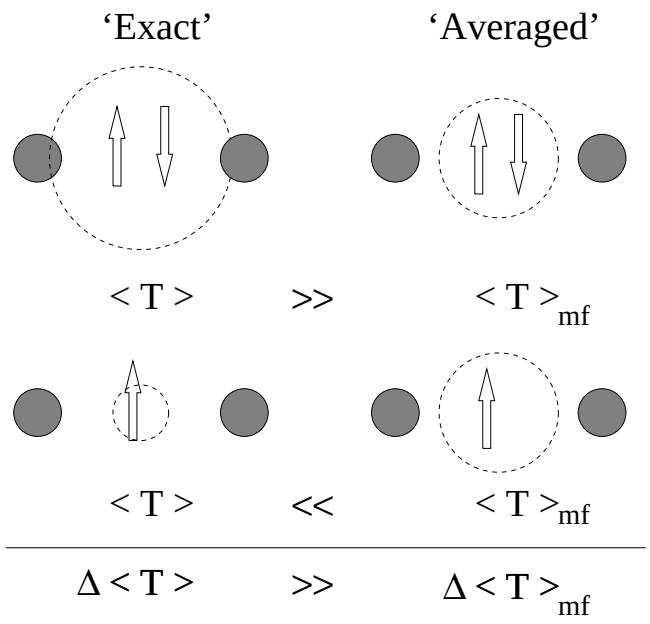

Fig. 7.1: Schematic representation of two-electron and single-electron wave function with (left column) and without (right column) taking into account the expansion of the hydrogen wave function.

explicitly. They cannot be treated in a mean field like way (as is done in band theory), taking an average orbital radius corresponding to the average occupation as determined from self-consistent calculations.

To model the effect of the "breathing" hydrogen we introduce an occupation-dependent hopping integral (following Hirsch [14]) between H and its nearest neighbours, besides the usual on-site Coulomb interaction of the Hubbard [15] or Anderson impurity [16] models. We consider the Hamiltonian of the form:

$$\begin{aligned} H &= -\Delta \sum_{\sigma} h_{\sigma}^{\dagger} h_{\sigma} + U h_{\uparrow}^{\dagger} h_{\uparrow} h_{\downarrow}^{\dagger} h_{\downarrow} \\ &- \sum_{\sigma} [\ (\ V_1 l_{\sigma}^{\dagger} h_{\sigma} h_{\bar{\sigma}}^{\dagger} h_{\bar{\sigma}} + V_2 l_{\sigma}^{\dagger} h_{\sigma} h_{\bar{\sigma}} h_{\bar{\sigma}}^{\dagger}\ ) + \text{H.c.}\ ], \end{aligned} \tag{7.1}$$

which describes the hybridization of a single hydrogen atom with a single ligand orbital. Here $h_{\sigma}^{\dagger}$ ($l_{\sigma}^{\dagger}$) creates an electron on the hydrogen (ligand), there is a charge transfer energy Δ between hydrogen and ligand (we assume $\Delta > 0$) and a Coulomb repulsion U between electrons on hydrogen. V_1 and V_2 are the occupation-dependent hydrogen-ligand hopping integrals. We discuss the first ionization energy E_- for photoemission on a single cell, consisting of a hydrogen atom and a ligand orbital, filled with two electrons. The minimum ionization energy E_- and the minimal electron affinity E_+ determine the excitation gap $E_{\text{gap}} = E_- - E_+$. An underestimation of the magnitude of E_- thus may lead to a too small gap energy, as seems to be the case in the LDA calculation for YH_3.

For simplicity we take $V_2 = 0$, so that the ground state of a single electron just corresponds to the electron being trapped in the collapsed hydrogen orbital, and has energy $-\Delta$. A straightforward calculation then gives the corresponding

ionization energy

$$E = \frac{U-\Delta}{2} - \sqrt{(\frac{U-\Delta}{2})^2 + 2V_1^2}.$$

Taking for simplicity $U = \Delta$ we obtain $E = -\sqrt{2}V_1$. The ionization energy thus is predominantly due to the loss of kinetic energy, because the single electron in the final state cannot escape from the collapsed hydrogen orbital. Therefore, the large gain in kinetic energy that was enabled for two electrons, is now impossible.
On the other hand, constructing a single-particle Hamiltonian with an averaged hopping integral $V_{\rm MF} \approx \langle h_\sigma^\dagger h_\sigma \rangle V_1$ and an "effective" on-site energy $\Delta_{\rm MF}$ (as it is done in an LDA calculation), the excitation energy would be simply the energy of the occupied mean-field orbital,

$$E_{\rm MF} = \frac{\Delta_{\rm MF}}{2} - \sqrt{(\frac{\Delta_{\rm MF}}{2})^2 + 2V_{\rm MF}^2}.$$

If the occupation of hydrogen $1s$ is significantly smaller than one per spin state, this approach will miss a large part of the kinetic energy contribution to the excitation energy, unless the "effective" on-site energy is corrected to take this effect into account.
In a mean-field treatment of this Hamiltonian, it will become apparent that the occupation-dependent hopping gives rise to very peculiar physics. Breaking down the conditional hopping terms into quadratic terms, we get: $l_\sigma^\dagger h_\sigma h_{\bar\sigma}^\dagger h_{\bar\sigma} \rightarrow l_\sigma^\dagger h_\sigma \langle h_{\bar\sigma}^\dagger h_{\bar\sigma}\rangle + \langle l_\sigma^\dagger h_\sigma\rangle h_{\bar\sigma}^\dagger h_{\bar\sigma}$. The first of these terms corresponds to weighting the "large" hybridization integral by the occupation of the hydrogen orbital, which is what one might have expected; the second term, however, is a correction to the on-site energy of hydrogen by a part of the kinetic energy. In this way, we obtain:

$$\begin{aligned} H_{\rm MF} &= \sum_\sigma [\, -\Delta_{\rm MF} h_\sigma^\dagger h_\sigma + (\, V_{\rm MF} l_\sigma^\dagger h_\sigma + \text{H.c.}\,)\,], \\ V_{\rm MF} &= V_1\, n_{\rm H} + V_2\,(1-n_{\rm H}) \\ -\Delta_{\rm MF} &= -\Delta + U\, n_{\rm H} + \alpha \langle T\rangle \\ \alpha &= \frac{V_1 - V_2}{V_{\rm MF}} \end{aligned} \tag{7.2}$$

where $n_h = \langle h_\sigma^\dagger h_\sigma\rangle$ and $\langle T\rangle$ is the energy of hybridization between hydrogen and ligand. We thus find the surprising result that in this approximation the expectation value of the kinetic energy $\langle T\rangle$ enters as an additional "potential" on the hydrogen sites, and is in fact even enhanced by the factor α. In the limit $V_1 \gg V_2$ we find $\alpha \rightarrow n_{\rm H}^{-1} > 1$, so that the correction to the on-site potential of hydrogen becomes $(V_1/V_{\rm MF})\langle T\rangle$, i.e. the kinetic energy for mixing with

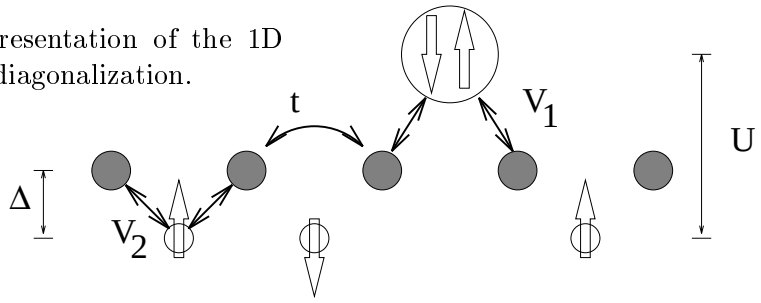

Fig. 7.2: Schematic representation of the 1D model used in the exact diagonalization.

the hydrogen site, but calculated with the hopping integral for the "expanded" atom. This is a huge energy, but it has a clear physical interpretation: for two electrons in the cell, the hydrogen atom will oscillate between H^0 and H^-, to take maximum advantage of the expansion of the wave function, and the hybridization energy will be large. Removing one electron, the remaining electron will essentially be trapped in the "collapsed" hydrogen orbital, and there is practically no more hybridization energy. In the mean-field wave function both electrons are in the lower molecular orbital, which (due to its strongly negative effective on-site energy resulting from Eq. 7.2) has predominant hydrogen character. The ionization energy, which by Koopmans' theorem should be given by the mean-field eigenvalue, then contains almost the entire kinetic energy of the two-electron state, because this kinetic energy has been put into the on-site potential of the hydrogen atom.

To make this more quantitative, we have performed exact diagonalization calculations for a one-dimensional (1D) chain of a model with occupation-dependent hybridization between hydrogen and ligand. A schematic representation of the model is given in Fig. 7.2. Computer memory and CPU time limitations prohibit the diagonalization of chains longer than six unit cells within this model, at least for the most interesting densities near two electrons per unit cell. For the given parameters, the ground state of this system corresponds closely to a state with two electrons in a local singlet state in each unit cell, with one electron primarily on H and the other primarily on the neighbouring ligands. Such a state is reminiscent of a Kondo-lattice insulator ground state. Figure 7.3 shows the **k**-resolved electron addition and removal spectra for the six-site chain at half-filling. To get a feeling for the dispersions of the different bands, we have combined spectra calculated with both periodic and antiperiodic boundary conditions. While there is no rigorous proof for this, inspection of Fig. 7.3 shows that in this way one obtains remarkably smooth "band structures". Unlike spectra obtained in e.g. the Hubbard model at half-filling, the calculated spectra are surprisingly "coherent": the spectral weight is largely concentrated in just three well defined "bands". In inverse photoemission there is a band of predominant metal character, with little dispersion. In photoemission, there is a strongly dispersive band of mixed hydrogen-metal character, and a dispersionless low intensity band of practically pure hydrogen character. More detailed

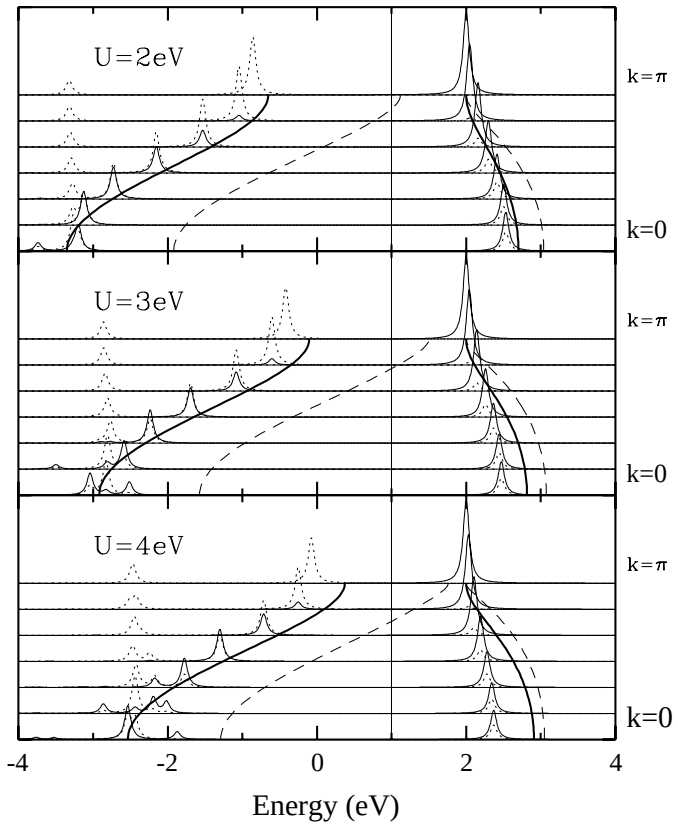

Fig. 7.3: Single particle spectral function of the 1D model with six unit cells. The part to the right (left) of the thin vertical line correspond to electron addition (removal) from the half-filled ground state (i.e. two electrons per unit cell). The full line corresponds to electron removal or addition on the "metal" sites, the dashed line to hydrogen. Parameter values are $V_1 = 2$ eV, $V_2 = 0.2$ eV, $t = 0.5$ eV, $\Delta = 1$ eV (see Fig. 7.2). The full (dashed) dispersion curve gives the mean-field bands calculated with (without) the correction $V_T = \alpha\langle T\rangle$.

analysis shows, that the dispersionless band corresponds to H^+ final states (i.e. it is a kind of "lower Hubbard band") whereas the dispersive band corresponds to H^0-like final states. Next, Fig. 7.3 shows the spectral function for different values of U. For comparison, the bands obtained by a mean-field solution of the model are also shown. The calculation has been done both with and without the kinetic energy correction $V_T = \alpha\langle T\rangle$ to the hydrogen on-site potential. Obviously, the calculation with V_T reproduces the exact band structure very well. Without V_T, the calculation still gives roughly the correct dispersion of the bands, but it substantially underestimates the gap size. As explained above, we believe that LDA misses the kinetic energy correction V_T, so that the LDA band structure rather corresponds to the bands without V_T. In a phenomenological way, this suggests a kind of "scissors operator" approach to obtain the "correct" band structure of YH_3 from the LDA result.

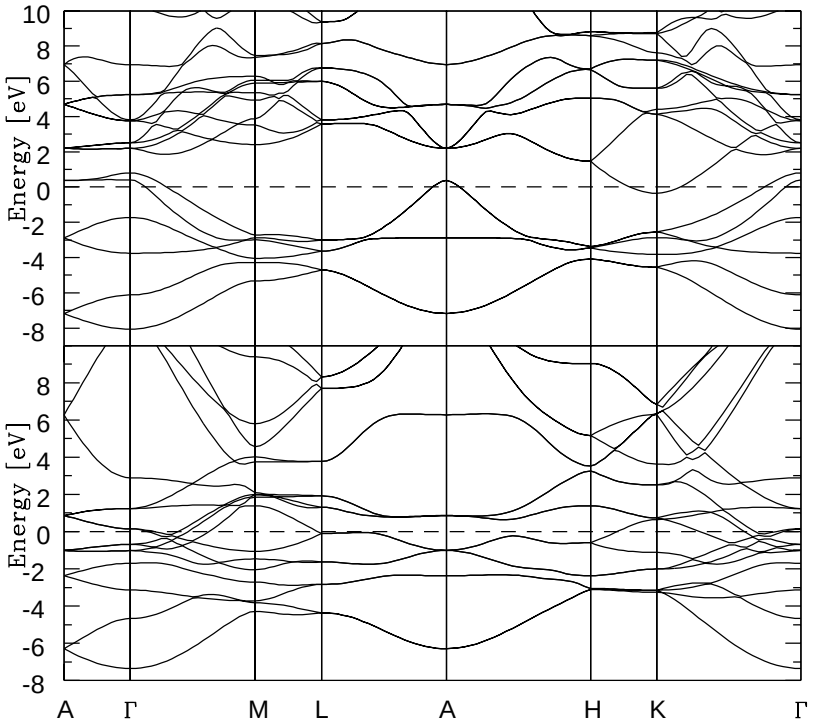

Fig. 7.4: Band structure of YH_3 (top) and metallic yttrium with the lattice constants of YH_3 (bottom). The Fermi energy is marked by the dashed line.

7.3 Application to YH_3

We now use the above ideas for the case of YH_3 and attempt to obtain reasonable parameters and subsequent estimates of the band gap. The three $4d$ electrons of Y will in the above scenario all be bound by the three H atoms per Y; this would again result in an insulating ground state. First, we obtain good estimates for the average hopping integrals and on-site energies, using a tight binding fit to an LDA band structure calculated with the LMTO method [17]. The basis set for the valence electrons consisted of $5s$-, $5p$-, $4d$, and $4f$-like basis functions for Y, and $1s$-, $2p$, and $3d$-like basis functions for H. The unit cell contained two empty spheres, with $1s$, $2p$, and $3d$-like basis functions. The upper panel of Fig. 7.4 shows the band structure calculated for YH_3 in the LaH_3 structure, which is practically identical to previous published results [2, 3]. In the lower panel we show the result of a calculation for Y metal with the lattice constants of YH_3, in order to establish the contribution of the H-$1s$ orbitals.

The lowest two bands, which have predominant $5sp$ character, are nearly identical in both calculations. Obviously, these free-electron-like states are not affected significantly by the insertion of hydrogen into the interstitial sites. In yttrium metal, the next group of states are the Y-$4d$ bands, which form a dense continuum with a width of ~ 6 eV. The Fermi energy cuts into the lower part

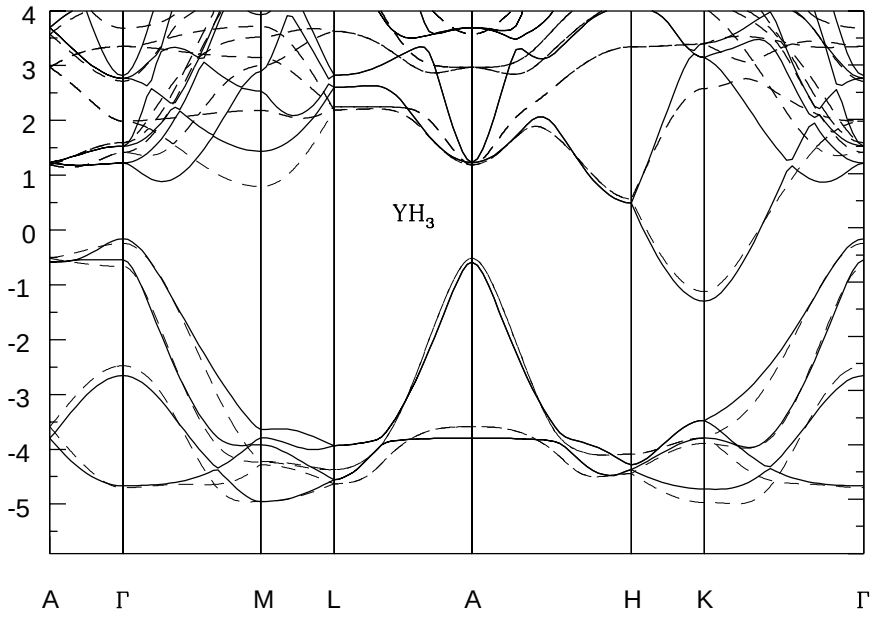

Fig. 7.5: LDA band structure for YH_3 (full line) and tight binding fit (dashed line). Energies are in eV.

of this complex of d bands. In YH_3 the situation is very different: the lowest Y-4d band (which is still quite reminiscent of the third-lowest band in metallic yttrium) is split off from the remaining d bands by ~ 4 eV, and in the resulting gap bands of predominantly hydrogen character are inserted. Although these hydrogen bands do have an appreciable width, they barely overlap with the lowermost of the following d bands. In fact, the band structure of YH_3 already shows a clear "gap" between the top of the hydrogen like valence band and the Y-4d-like conduction band throughout the entire Brillouin zone—YH_3 thus is already "almost" a semiconductor. The Fermi energy cuts into the top of the hydrogen-like valence band and the bottom of the d-like conduction band, so that LDA predicts YH_3 to be a semimetal. The shift of the lowermost d to considerably higher binding energy upon insertion of hydrogen, which is predicted by LDA, is in qualitative agreement with the photoemission data of Fujimori and Schlapbach [18]: for metallic yttrium, these authors found a high intensity structure at binding energies ≤ 2 eV, which probably corresponds to the occupied part of the Y-4d bands. For YH_3 a similar structure occurs at a binding energy of 6 eV, indicating the shift of the d band away from E_F. However, the lowest Y-4d is centered at around -4 eV, which means that the experimental shift is about 2 eV larger than predicted by LDA. The picture thus is quite reminiscent of the well-known band-gap problem in semiconductors, where LDA fails to give correct values for the semiconducting gaps.

To extract additional information, we performed a tight-binding fit to the LDA band structure. The fit was made with a basis of Y-s,-p,-d and H-s orbitals,

Y-H_1		Y-H_2		Y on-site		H on-site	
$(ss\sigma)_1$	-1.2	$(ss\sigma)_2$	-1.1	$E_{s,Y}$	9.3	E_{s,H_1}	-0.4
$(sp\sigma)_1$	2.6	$(sp\sigma)_2$	2.9	E_p	28.1	E_{s,H_2}	-0.3
$(sd\sigma)_1$	-2.0	$(sd\sigma)_2$	-1.6	$E_{yz,zx}$	1.8		
				E_{xy,x^2-y^2}	2.8		
				$E_{3z^2-r^2}$	0.6		

Table 7.1: Y-H hopping integrals and on-site energies obtained from a tight binding fit to the LMTO band structure of YH_3. All values are in eV. The indices 1 and 2 refer to hydrogen atoms in the metal plane and in tetrahedral sites, respectively.

with a crystal field splitting of Y-d, and considering only nearest-neighbour hopping integrals. Fig. 7.5 shows that this approach leads to a surprisingly good fit of the first few valence and conduction bands. Table 7.1 contains the fit parameters that are most relevant for our discussion.

We will now use the results of the fit to determine some parameters for an Anderson-impurity like calculation between H-1s and Y-4d states. For simplicity, this calculation considers only the hybridization between H-1s and Y-4d orbitals. This is a reasonable approximation, because the bands near the Fermi level are of primarily H-1s character, and the largest mixing is with the Y-4d states. This is also according to the parameters of Table 7.1: the mixing is approximately proportional to the hopping integral divided by the difference in on-site energies. Clearly, $(ss\sigma)/(E_d - E_{s,H})$ is much larger than $(sp\sigma)/(E_d - E_{p,H})$ and $(ss\sigma)/(E_d - E_{s,H})$. Because the tight binding calculation does not fit the LDA band structure at high energies, there are some uncertainties in the magnitudes of the fit parameters, especially in the position of the Y-4p band. However, it turned out that the parameters that we will use, i.e. the H-1s–Y-4d hopping integrals and the on-site energy difference $E_d - E_{s,H}$, are not much affected by the choice of the other parameters.

We can now compare the tight binding Hamiltonian to the impurity Hamiltonian

$$\begin{aligned} H &= \sum_{\mathbf{k},\nu,\sigma} \epsilon_\nu(\mathbf{k}) d^\dagger_{\mathbf{k},\nu,\sigma} d_{\mathbf{k},\nu,\sigma} + \sum_{j,\sigma} \tilde{\epsilon}_j h^\dagger_{j,\sigma} h_{j,\sigma} \\ &+ \sum_{i,j,\sigma} [\ (\ V^{(1)}_{(i,\nu),j} d^\dagger_{i,\nu,\sigma} h_{j,\sigma} h^\dagger_{j,\bar{\sigma}} h_{j,\bar{\sigma}} + V^{(2)}_{(i,\nu),j} d^\dagger_{i,\nu,\sigma} h_{j,\sigma} h_{j,\bar{\sigma}} h^\dagger_{j,\bar{\sigma}}\ ) + \text{H.c.}\ ] \\ &+ U \sum_j h^\dagger_{j,\uparrow} h_{j,\uparrow} h^\dagger_{j,\downarrow} h_{j,\downarrow} \end{aligned} \tag{7.3}$$

in a mean field way. Here, $\epsilon_\nu(\mathbf{k})$ denotes the Y-4d bands, as obtained from the tight-binding fit.

In a mean-field treatment, Eq. (7.3) would turn into

$$\begin{aligned} H &= \sum_{\mathbf{k},\sigma} \epsilon_\nu(\mathbf{k}) d^\dagger_{\mathbf{k},\nu,\sigma} d_{\mathbf{k},\nu,\sigma} + \sum_{j,\sigma} \Delta_j h^\dagger_{j,\sigma} h_{j,\sigma} \\ &+ \sum_{i,j,\sigma} [\ (\ V^{(1)}_{(i,\nu),j} d^\dagger_{i,\nu,\sigma} h_{j,\sigma} n_j + V^{(2)}_{(i,\nu),j} d^\dagger_{i,\nu,\sigma} h_{j,\sigma}(1-n_j)\ ) + \text{H.c.}\ ], \quad (7.4) \end{aligned}$$

with $n_j = \langle h^\dagger_{j,\uparrow} h_{j,\uparrow} \rangle = \langle h^\dagger_{j,\downarrow} h_{j,\downarrow} \rangle$ and $\Delta_j = \tilde{\epsilon}_j + U n_j$. We now introduce the parameter λ, which we assume independent of j, as $\lambda = V^{(1)}_{(i,\nu),j} / V^{(2)}_{(i,\nu),j}$, i.e. the ratio of hopping integrals for the collapsed and expanded hydrogen atom. We then estimate the change as

$$V^{\text{TB}}_{(i,\nu),j} \approx (n_j + \lambda(1-n_j)) V^{(1)}_{(i,\nu),j}, \quad (7.5)$$

where $V^{\text{TB}}_{(i,\nu),j}$ is the hybridization integral extracted from the tight-binding fit. Since n_j can be obtained from the tight-binding calculation as well, we can thus, for given λ, obtain an estimate of $V^{(1)}_{(i,\nu),j}$. Next, we estimate the "bare" on-site energies ϵ_j of the hydrogen atoms from those of the tight-binding fit, Δ^{TB}_j, as follows:

$$\epsilon_j = \Delta^{\text{TB}}_j - n_j U. \quad (7.6)$$

This introduces another unknown parameter: the on-site Coulomb repulsion U between two electrons on the hydrogen site. While an ab-initio calculation of U and λ would be highly desirable, this is outside the range of techniques available to us. We therefore will treat these quantities as implicit parameters, and consider the variation of possible results when U and λ are varied within "reasonable bounds".

Using the parameters estimated in this way, we now proceed to an impurity-like calculation to determine the stabilization energy of Kondo-like local singlets, formed on a single hydrogen atom in the lattice of Y-4d orbitals. In the first step, we calculate the ground state energy $E^{(2)}_0$ of a two-electron bound state from the *ansatz*

$$|\Psi^{(2)}\rangle = [\ \alpha h^\dagger_\uparrow h^\dagger_\downarrow + \frac{1}{\sqrt{2}} \sum_{\nu,\mathbf{k}} \beta_\nu (\ d^\dagger_{\mathbf{k},\nu,\uparrow} h^\dagger_\downarrow + h^\dagger_\uparrow d^\dagger_{\mathbf{k},\nu,\downarrow}\ )\ ] |\text{vac}\rangle.$$

Here summation over $\mathbf{k}$ and ν refers to the Y-4d bands. The dispersion of these bands and the hybridization matrix elements between the band states and the hydrogen atom are calculated using the parameters from the tight binding fit, with the hydrogen-yttrium hybridizations depending on λ and the hydrogen on-site energy on U. Then, we want to know the stability of this state against decay into a state with a single electron remaining in the hydrogen atom, and

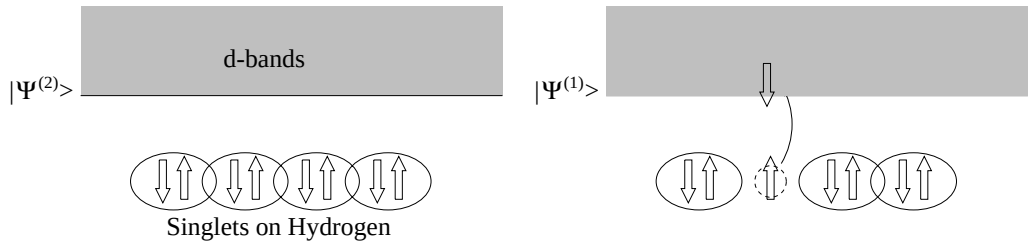

Fig. 7.6: Schematic representation of the stabilization energy for the local two-electron bound state.

the second electron being in a free yttrium d-like state. The energy $E_0^{(1)}$ of the single electron in the hydrogen is calculated from the ansatz

$$|\Psi^{(1)}\rangle = [\ \alpha' h_\uparrow^\dagger + \sum_{\nu,\mathbf{k}} \beta'_\nu d^\dagger_{\mathbf{k},\nu,\uparrow}\ ]|\mathrm{vac}\rangle,$$

and for the energy of the d-like electron we simply choose the lower bound of the d-band complex, E_{edge}. We then form the difference $\Delta E = E_0^{(2)} - (E_0^{(1)} + E_{\mathrm{edge}})$ (see Fig. 7.6), which obviously determines the stability of the two-electron state against decay. This energy will be a function of the unknown parameters U and λ. The result then is shown in Fig. 7.7.

One can see that for "reasonable" values of U and not very extreme values of λ the two-electron bound state attains a stabilization energy of several electronvolts. Drawing an analogy with the situation in cuprate superconductors, where the Zhang-Rice singlet has a stabilization energy of approximately 1 eV, it seems quite reasonable to adopt the picture of local bound states. Then, for YH_3 one may expect that these bound states form a split-off band, with the Fermi energy lying in the gap between these states and the bottom of the $4d$ band; the physics is similar to our exact result on the 1D cluster.

7.4 Doping dependence of the electronic structure

To simulate the physics of what happens as one removes hydrogen from YH_3, we resort to an exact calculation of a small cluster as done above, but we now remove one hydrogen site and one electron. In Fig. 7.8 we show the spectral function for electron removal and electron addition before and after removal of the hydrogen. In the top panel, one can clearly recognize the large gap between the hydrogen like valence band and the metal like conduction band. Upon hydrogen removal, as shown in the bottom panel, the Fermi energy jumps into the metal band, which implies that hydrogen behaves like an H^- ion in that it binds two electrons. This is consistent with the above discussion and also suggested by Ng *et al* [11].

In our previous discussion we came to the conclusion that H actually binds two electrons: one localized on H, and the other on the nearest-neighbour metal

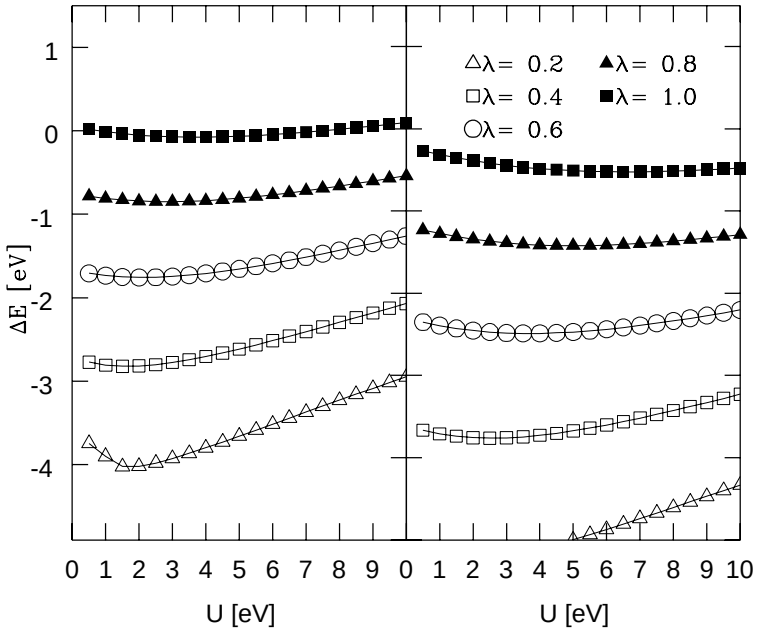

Fig. 7.7: Ionization energies ΔE calculated with the impurity model for the metal plane hydrogen (left panel) and the tetragonal hydrogen (right panel). Note that the other tight binding parameters depend on the values for U and λ through Equations (7.5) and (7.6).

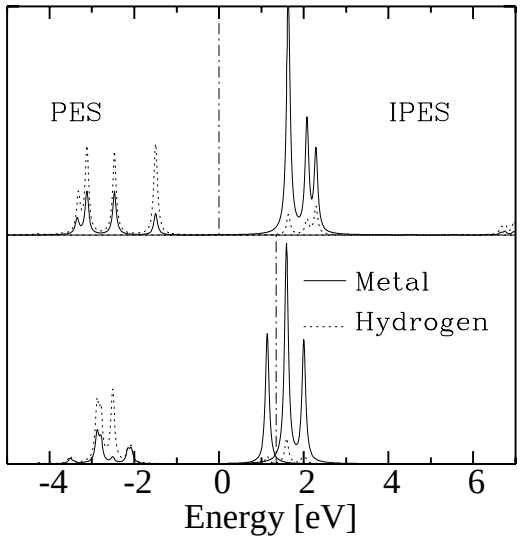

Fig. 7.8: Single particle **k**-integrated spectral function for a three unit cell cluster of the 1D model with open boundary conditions. The spectra are calculated at "half-filling" (upper part) and with one charge neutral hydrogen atom removed from the central cell (lower part). The parts of the spectra to the right (left) of the vertical dashed-dotted line correspond to electron addition (removal). Parameter values are $\Delta = 1$ eV, $U = 2$ eV, $t = 0.5$ eV, $V_1 = 2$ eV, $V_2 = 0.2$ eV.

atoms. With the removal of a H atom, which takes only one electron with it, another "lonely" electron is left behind, which must then be in the conduction band. Removal of H from the trihydride insulator should then transfer spectral weight for electron removal from the top of the valence band to the bottom of the conduction band, some 2 eV higher in energy. This kind of behaviour upon doping is very similar to that predicted for [19] and observed [20] in the high T_c cuprates. Consistent with this are the observations by Peterman *et al.* [7], who found that in hydrogen depleted trihydrides the Fermi energy falls into a "band" with very weak spectral weight, which grows upon further depletion.

7.5 Conclusions

We have shown that hydrogen is an extreme example of an atom with a large orbital occupation dependence of the orbital radius, leading to large occupation-dependent hopping integrals in hydrides. We argue that explicit inclusion of such terms in the Hamiltonian results in a "scissors operator" like separation of the valence and conduction bands and, consequently, the opening of a substantial gap. We argue that the insulating character of YH_3 can be understood in this way. Using reasonable parameters obtained from tight binding fits to the band structure, we find that the ground state of YH_3 corresponds closely to that of a Kondo insulator, with each H binding two electrons in a singlet state.

References

[1] J. N. Huiberts, R. Griessen, J. H. Rector, R. J. Wijngaarden, J. P. Dekker, D. G. de Groot, and N. J. Koeman, Nature **380**, 231 (1996)

[2] Y. Wang and M. Y. Chou, Phys. Rev. Lett. **71**, 1226 (1993)

[3] J. P. Dekker, J. van Ek, A. Lodder, and J. N. Huiberts, J. Phys. Cond. Mat. **5**, 4805 (1993)

[4] N. F. Miron, V. I. Shcherbak, V. N. Bykov, and V. A. Levdik, Sov. Phys. Crystallogr. **17**, 342 (1972)

[5] T. J. Udovic, Q. Huang, and J. J. Rush, J. Phys. Chem. Solids **57**, 423 (1996)

[6] P. J. Kelly, J. P. Dekker, and R. Stumpf, Phys. Rev. Lett. **78**, 1315 (1997)

[7] D. J. Peterman, J. H. Weaver, and D. T. Peterson, Phys. Rev. B **23**, 3903 (1981)

[8] M. Gupta and J. P. Burger, Phys. Rev. B **22**, 6074 (1980)

[9] N. I. Kulikov and A. D. Zvonkov, Z. Physiol. Chem. N. F. **117**, 113 (1979)

[10] N. I. Kulikov, J. Less-Common Met. **88**, 307 (1982); *ibid.***107**, 111 (1985)

[11] K. K. Ng, F. C. Zhang, V. I. Anisimov, and T. M. Rice, Phys. Rev. Lett. **78**, 1311 (1997)

[12] D. A. McQuarrie and P. A. Rock, *General Chemistry* (W. H. Freeman & Co., New York, 1984)

[13] H. T. Jonkman and P. van Duijnen, private communication

[14] J. E. Hirsch, Phys. Rev. B **48**, 3327 (1993)

[15] J. Hubbard, Proc. R. Soc. London Sect. A **276**, 238 (1963)

[16] P. W. Anderson, Phys. Rev. **124**, 41 (1961)

[17] O. K. Andersen, Phys. Rev. B **12**, 3060 (1975); O. K. Andersen and O. Jepsen, Phys. Rev. Lett. **53**, 2571 (1984); O. K. Andersen, O. Jepsen, and D. Glötzel, in *Highlights of Condensed-Matter Theory*, edited by F. Bassani, F. Fumi, and M.P. Tosi (North-Holland, New York, 1985)

[18] A. Fujimori and L. Schlapbach, J. Phys.C: Solid State Phys. **17**, 341 (1984)

[19] H. Eskes, M. B. J. Meinders, and G. A. Sawatzky, Phys. Rev. Lett. **67**, 1035 (1991)

[20] C. T. Chen, F. Sette, Y. Ma, M. S. Hybertsen, E. B. Stechel, W. M. C. Foulkes, M. Schluter, S-W. Cheong, A. S. Cooper, L. W. Rupp, Jr., B. Batlogg, Y. L. Soo, Z. H. Ming, A. Krol, and Y. H. Kao, Phys. Rev. Lett. **66**, 104 (1991)